

## STM-induced formation of Ag islands on Ag(111)

J.E. Freund, M. Edelwirth, J. Grimming, R. Schloderer, W.M. Heckl

Institut für Kristallographie und Mineralogie der Universität München, Theresienstrasse 41, D-80333 München, Germany  
 (Fax: +49-89/2394-4331, E-mail: W. Heckl@lrz.uni-muenchen.de)

Received: 25 July 1997/Accepted: 1 October 1997

**Abstract.** The formation of triangular-shaped adatom islands and vacancy islands on Ag(111) at room temperature is observed in a local growth experiment. The tip of a scanning tunneling microscope (STM) vibrating normal to the surface leads to a local modification. Atoms are removed from flat terraces and renucleate as adatom islands. Simultaneously with the modification process the surface is imaged with the STM. In the case of triangular islands only one out of two possible types of close-packed (110) step edges is found in the STM images. This observation is explained by differences in the step formation energy, rather than by diffusion.

The homoepitaxial growth of metal atoms on (111) surfaces has been studied from various aspects, both experimentally and theoretically. Besides the fundamental understanding of the involved atomic processes the main interest stems from the technologically important control of layer-by-layer growth. Layers are usually grown by molecular beam deposition techniques (MBE) in which material from the gas phase nucleates on the substrate.

The temperature dependence of island growth has been investigated for the deposition of Pt on Pt(111) by Michely et al. [1]. The authors found a rich variation of growth modes, from fractal growth for low temperatures to various types of triangular and hexagonal island shapes at different elevated temperatures. For coverages exceeding one monolayer Kunkel et al. [2] reported a layer-by-layer growth regime for  $T > 600$  K. In the case of Ag/Ag(111), however, no layer-by-layer growth was observed in the temperature range between 175 K and 575 K [3]. However, a smooth layer growth can be generated either by precovering the surface with a submonolayer of Sb [3] or by an artificially high island density, produced for example by short sputter pulses [4].

Theoretical work to elucidate growth processes on stepped (111) surfaces has investigated the step formation energies and diffusion along or perpendicular to steps. Stumpf and Scheffler [5] have performed density-functional calculations elucidating the formation energy of densely packed steps on Al(111). The calculations show a difference of 0.016 eV for

the two different types of step along the (110) directions (Fig. 1). Island morphologies are often explained by kinetic processes. Interlayer mass transport on Ag(111) has been studied in detail by Li and DePristo [6], revealing a strong anisotropy between the two different types of densely packed step edges.

Recently the formation of vacancy islands on Ag(111) has been reported by applying a higher tunneling current (gap resistance  $R = 0.1$  M) [7]. In that experiment the STM tip was fixed at a certain position for 60 s and induced islands were observed by subsequent imaging.

Here we report the growth of Ag islands on a flat Ag surface initiated by an STM tip vibrating normal to the surface. The STM is used to initiate the atom transport process as well as simultaneously imaging the surface. Ag atoms are removed from the surface and nucleate again along crystalline axes. No additional Ag atoms are added from the gas phase. All of the redistribution processes and the imaging occur at the

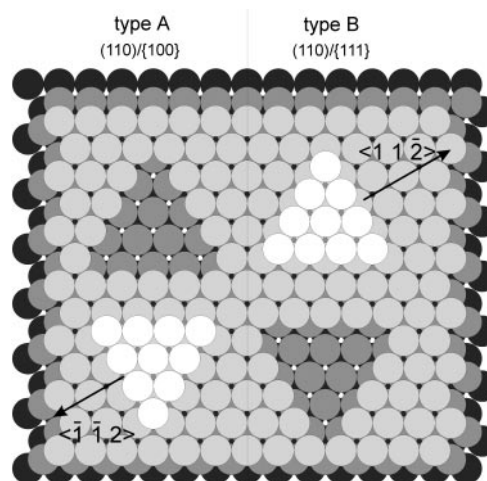


**Fig. 1.** On the (111) surface of an f.c.c. packed lattice two non-equivalent types of step edges are possible, forming either {100} facets (type A) or {111} facets (type B). Vacancy islands are rotated by 180° relative to the adatom islands within the same type of steps

STM operating temperature, which was 295 K. Triangular islands are observed on Ag(111) with only one type of island boundary. We show that this effect can be understood in terms of different step formation energies rather than by different diffusion velocities.

## 1 Experimental

The experiments were performed in a UHV chamber equipped with facilities for STM, low-energy electron diffraction (LEED) and Auger electron spectroscopy (AES). During STM measurements the chamber is pumped with an ion sublimation pump maintaining a base pressure of  $2 \times 10^{-10}$  mbar. The STM is a slightly modified commercial instrument [8] with home-built analog electronics. STM images are recorded on video tape. Because the tip was vibrated at 400 Hz in the  $z$ -direction in order to achieve a surface modification, the scanning frequency was limited to 3 lines per second. The vibration amplitude was chosen such that the tunneling current reached several tens of nA to 100 nA at the minimum tip-surface distance and dropped to a value of less than 10 pA at the maximum tip-surface distance. The average current was held constant at values between 100 pA and 1.5 nA. Considering a logarithmic distance dependence of 3 Å per order of magnitude for the STM current the vibration amplitude is estimated as  $\approx 10$  Å. The typical tunneling voltage for all images was 1 V. The feedback cutoff frequency was well below the vibration frequency but high enough to image steps in an 'average constant current mode'.

Scanning at 3 lines/s and recording 512 pixels/line together with a vibration amplitude of 400 Hz leads to a modulation of about 4 pixels length along the scan lines. This frequency was partly eliminated before recording the image by first-order low-pass filtering with a cutoff frequency of 20 Hz. Although this treatment leads to an artificial smoothing of steps it is necessary for recording STM images. All images were obtained with etched W-tips.

The Ag single crystal was cut with high precision parallel to the (111) plane. After inserting it into UHV it was annealed at 970 K for 3 h to remove surface damage from the polishing treatment. The surface was then cleaned by several cycles of sputtering (15 min, 300 K, 700 eV  $\text{Ar}^+$ ) and annealing (10 min, 1020 K, slow cooling down to 720 K at 20 K/min). The surface purity was checked by AES; LEED measurements showed sharp diffraction patterns.

## 2 Results

Scanning on Ag(111) with the tip vibrating in the  $z$ -direction continuously modifies the surface. Figure 2 shows the third scan of an area ( $2500 \text{ \AA} \times 2500 \text{ \AA}$ ) which in the first scan only exhibited the horizontal double step in the middle and the diagonal features in the right half of the image. The formerly flat terraces show various vacancy islands (darker) and adatom islands (brighter). The side length of the islands is of the order of several hundred angstroms. Both kinds of island have predominantly triangular shapes. However, the vacancy islands are rotated relative to the adatom islands by  $180^\circ$ . Tip effects can be excluded for imaging faults as well as for

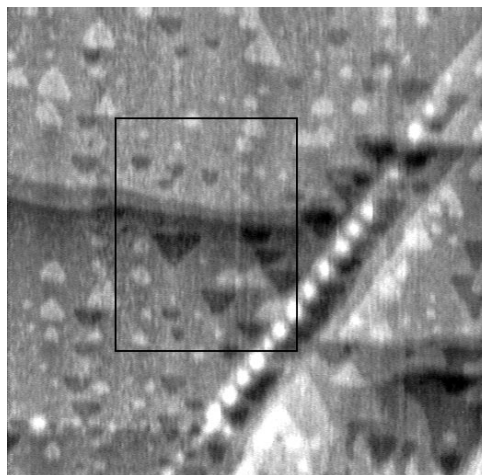


**Fig. 2.**  $2500 \text{ \AA} \times 2500 \text{ \AA}$  STM image of the Ag(111) surface after the third scan on the same area. Tunneling parameters:  $U_T = 1 \text{ V}$ ,  $I_{T(\text{average})} = 1 \text{ nA}$

the cause of triangle formation, since the line scan process is equivalent in both directions, forward and backward.

The STM images in Fig. 3a,b show two consecutive scans of a detail of Fig. 2 with an area of  $1250 \text{ \AA} \times 950 \text{ \AA}$ . The structural changes are clearly visible. Both adatom and vacancy islands tend to grow and neighboring islands coalesce, mainly retaining their triangular forms. More than one layer deep holes can also be observed, for instance in the middle of Fig. 3b (marked by an arrow), which is still smaller in Fig. 3a and is missing completely in Fig. 2. The depth of the defects is increasing up to several layers after continuous scanning.

The high resolution of Fig. 3b shows that most islands are not pure triangles but strongly asymmetric hexagons with one set of triangular step edges much longer than the other. The ratio between long and short edges was not always constant (Fig. 4). In fact, in several cases regular hexagonal islands were observed. The shape, however, remained constant for all islands which were generated after the same sputter/annealing cycle. A possible explanation may be a small difference in the crystal annealing parameters. Mainly hexagonal islands at room temperature have been reported by Meyer and Behm [9] for sputter defects as well as for Ag islands originating from vapor deposition.

With the technique used, modifications are observed by comparing consecutive images. The modification process, however, takes place continuously while scanning and imaging. This can account for the slightly round shapes of several step edges at higher resolution in 3a,b. The fuzziness of the Ag step edges, which has been reported in the literature [10, 11], has not been observed because of the lower resolution in the vibration mode. An improvement in the resolution could be reached by first modifying the surface in the vibrating STM mode, followed by imaging under the usual conditions. A limitation in the resolution due to tip damage caused by vibration cannot be excluded.

## 3 Discussion

The different orientations of trigonal adatom and vacancy islands can be traced back to the threefold symmetry of the f.c.c. (111) surface, as has been shown, for example, in the

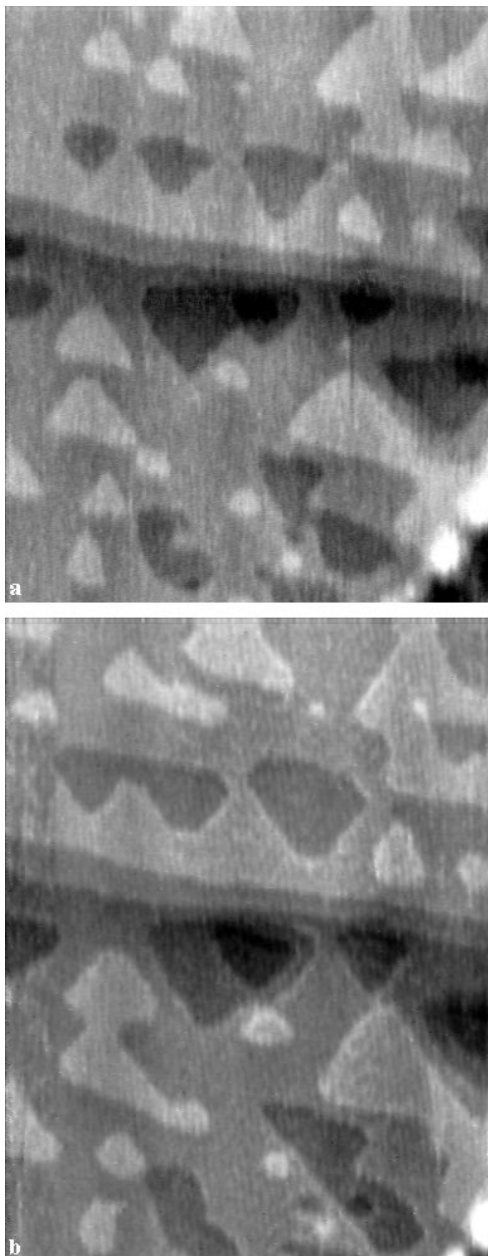


**Fig. 3.** The two scans of the area indicated by the rectangle in Fig. 2. The size is  $1250 \text{ \AA} \times 950 \text{ \AA}$

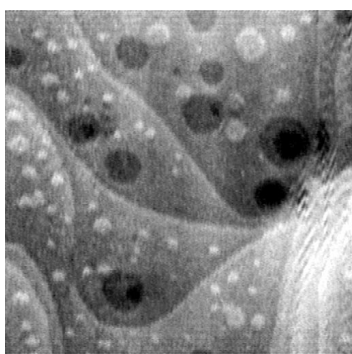


**Fig. 4.**  $2000 \text{ \AA} \times 2000 \text{ \AA}$  STM image of the Ag(111) surface. The islands are generated in the vibrating STM mode after a different sputter/annealing cycle than those imaged in Fig. 3

case of Pt(111) [12]. Close-packed step edges are oriented along the  $\langle 110 \rangle$  directions. However, two different types of  $\langle 110 \rangle$  step edges are possible, forming either  $\{100\}$  or  $\{111\}$  microfacets corresponding to a step down direction in either the  $[\bar{1}\bar{1}2]$  direction or the opposite direction (Fig. 1). The steps are often defined as  $\langle 110 \rangle / \{100\}$  and  $\langle 110 \rangle / \{111\}$  steps and will be denoted here as type A and type B respectively. Since the triangular vacancy islands are rotated relative to the adatom islands, it is obvious from Fig. 1 that one type of step dominates. Two possible causes for this phenomenon will be discussed in the following: interlayer mass transport and step formation energies.

Mass transport processes on a (111) metal surface can be classified into three categories. First, on a flat terrace two-dimensional diffusion is not hindered at room temperature. Diffusion perpendicular to steps, however, must cross a potential energy barrier (PEB). Li and DePristo [6] have calculated this barrier for Ag(111). They found for the favored exchange diffusion process across a perfect A-type step a PEB of 0.31 eV, but only a 0.06 eV PEB for the B-type step. In the case of a 19 atom hexagon the relative difference was even more pronounced, with PEB values of 0.22 eV and 0.02 eV respectively. These results imply a relatively free diffusion across B-type steps at room temperature, whereas from A-type steps the major fraction of adatoms should be reflected. The third important path is the diffusion along step edges. Michely et al. [1] found a temperature-dependent difference for the migration velocities along A- and B-type steps on Pt(111). In the low-temperature regime ( $T < 450 \text{ K}$ ) the diffusion coefficient is larger for A-type steps. Assuming that this behavior also holds for Ag(111), and taking into account the difference in the PEB, we will now examine the implications for the formation of adatom and vacancy islands.

Let us consider a hexagonal vacancy island which contains both types of step (Fig. 5a). Adatoms diffusing on the surrounding terrace will easily cross the B-type steps, and since migration along them is smaller than on A-type steps the sticking probability on B-type steps is further enhanced. A higher adatom density leads to a higher probability for the nucleation of a new step edge line and thus to a growth perpendicular to the B-type steps. Adatoms diffusing on the defect island will increase this effect. Once they reach a step they will migrate along the step, and the lower the migration speed the higher the density of step adatoms. For defect islands diffusion will lead to a triangular form confined by B-type steps, as indicated in Fig. 5b. The same mechanisms applied to an adatom island (Fig. 5c) also lead to an advancement of B-type steps (Atoms diffusing on top of the island will cross B-type steps and will predominantly stick there. Atoms from the surrounding terrace will migrate more easily on A-type steps until they reach kink sites of B-type steps). However, since the island now grows outwards, a triangle with A-type steps is formed (Fig. 5d). If diffusion effects were the dominant formation mechanisms, defect and adatom islands should point in the same direction. This is not the case in the observed STM images.

Therefore we suggest differences in the step formation energy as the cause of the observed triangular islands. Assuming a linear energy dependence on the atom's coordination number results in equivalent energies for both types of step. Full density-functional theory calculations, however, reveal

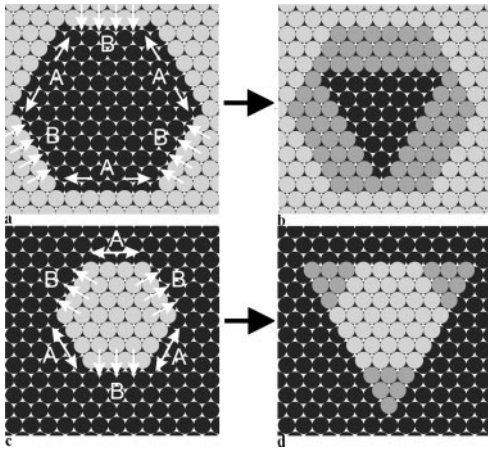


**Fig. 5a–d.** Diffusion effects applied to hexagonal islands. **a** A hexagonal defect island grows into a triangle by diffusion across the B-type steps and migration along the A-type steps **b** which is confined by B-type step edges. **c** A hexagonal adatom island is changed by the same mechanisms into a triangle with A-type steps, as sketched in **d**. Note that both resulting triangles point in the same direction with regard to the surface

an energy difference between the two step types. For Al(111), Stumpf and Scheffler [5] found step formation energies of 0.248 eV for the A-type and 0.232 eV for the B-type steps. Semiempirical embedded atom calculations show a similar trend for Ag(111) [13]. Therefore we conclude that the observed islands are mainly confined by B-type steps because of their lower formation energy. Since the observed islands have edge lengths of the order of several tens of atoms, the influence of corner positions is negligible. Steps of defect and adatom islands thus have the same topology, and the energy argument holds for both.

#### 4 Summary and outlook

The STM has been used as a surface modification tool by vibrating the tip perpendicularly to the surface with current maxima up to several tens of nA. Simultaneously, the scanned surface has been imaged by keeping the average tunneling current constant. On Ag(111), defect islands with triangular symmetry have been created by this technique. The removed

atoms nucleate again on other parts of the surface, forming adatom islands of the same symmetry. The depth of the defects increases to several monolayers after multiple scanning. Adatom and vacancy islands are predominantly confined by the same kind of step edge, presumably by  $\langle 110 \rangle / \langle 100 \rangle$  microfacets (type A). This observation can only be explained by a lower step formation energy than for steps forming  $\langle 110 \rangle / \langle 111 \rangle$  facets (type B).

The applied vibrating STM technique can be used to study surface growth without adding atoms by vapor phase deposition. It has the advantages of equal temperature for all modification and imaging processes (limited only by the STM operation temperature) and of a very short time delay between the formation of new surface features and their imaging.

Another field of application is the local structuring at monolayer level. Since the removed material renucleates along crystalline axes it should be possible to write positive as well as negative structures with one or multiple monolayer depth on surfaces with suitable pre-orientations. The method could be extended by not only scanning square fields but also by writing more complicated structures.

*Acknowledgements.* Financial support through Deutsche Forschungsgemeinschaft (He 1617/6-1) and Bayerisches Hochschulsonderprogramm II is gratefully acknowledged.

#### References

1. T. Michely, M. Hohage, M. Bott, G. Comsa: Phys. Rev. Lett. **70**, 3943 (1993)
2. R. Kunkel, B. Poelsema, L.K. Verheij, G. Comsa: Phys. Rev. Lett. **65**, 733
3. H.A. van der Vegt, H.M. van Pinxteren, M. Lohmerier, G. Comsa: Phys. Rev. Lett. **68**, 3335 (1992)
4. G. Rosenfeld, R. Servaty, C. Teichert, B. Poelsema, G. Comsa: Phys. Rev. Lett. **71**, 895 (1993)
5. R. Stumpf, M. Scheffler: Phys. Rev. Lett. **72**, 254 (1994)
6. Y. Li, A.E. DePristo: Surf. Sci. **319**, 141 (1994)
7. F. Mugele: *Stufenfluktuationen auf Ag(111)*, Dissertation, Konstanz, Germany (1997)
8. Park Scientific Instruments, VP
9. J.A. Meyer, R.J. Behm: Phys. Rev. Lett. **73**, 364 (1994)
10. J.F. Wolf, B. Vicenzi, H. Ibach: Surf. Sci. **249**, 233 (1991)
11. M. Dietterle, T. Will, D.M. Kolb: Surf. Sci. **327**, L495 (1995)
12. T. Michely, G. Comsa: Surf. Sci. **256**, 217 (1991)
13. R.C. Nelson, T.L. Einstein, S.V. Khare: Surf. Sci. **295**, 462 (1993)